[14]Y. Nagaoka, Phys. Rev. 138, A1112 (1965); Progr. Theor. Phys. **37**, 13 (1966).
[15]C. Y. Cheung and R. D. Mattuck, Phys. Rev. B **2**, 2735 (1970).
[16]A. A. Abrikosov, Physics (N.Y.) **2**, 61 (1965).
[17]Y. Kurata, Prog. Theor. Phys. **43**, 621 (1970); B. Kozarzewski, Acta Phys. Pol. A **40**, 553 (1971).
[18]J. A. Applebaum and J. Kondo, Phys. Rev. Lett. **19**, 906 (1967).
[19]M. T. Beal-Monod and R. A. Weiner, Phys. Rev. **170**, 552 (1968); Phys. Rev. B **3**, 145 (1971), and references therein.
[20]M. D. Daybell and W. Steyert, Phys. Rev. Lett. **18**, 398 (1967).
[21]H. Suhl, *Rendiconti della Suola Internazionale de Fisica 'Enrico Fermi* (Academic, New York, 1967), XXXVII Corso.

PHYSICAL REVIEW B VOLUME 7, NUMBER 7 1 APRIL 1973

Modified Zener Model for Ferromagnetism in Transition Metals and Alloys—Model Calculations of T_C *

L. C. Bartel
Sandia Laboratories, Albuquerque, New Mexico 87115
(Received 7 August 1972)

An essential feature of the modified Zener model for ferromagnetism in transition metals and alloys is the coupling of an itinerant d electron to a localized spin in accordance with Hund's rule. In contrast to the Stoner–Wohlfarth model for ferromagnetism, this model takes into account the Hund's-rule effects and the orbital degeneracy of the d electrons. The exchange-enhanced dynamic susceptibility is calculated, and from its singularity in the static long-wavelength limit, the Curie temperature T_C is calculated as a function of bandwidth, the exchange interactions, and the number of itinerant d electrons per atom where a fcc tight-binding density of states is assumed. The results of the model calculation of T_C are compared to results for a pure itinerant-electron ferromagnet of the Stoner–Wohlfarth type and compared to experimental results for T_C as a function of pressure. The calculated T_C is found consistent with the experimental data. The unusual excitation spectrum for the modified Zener model is also discussed.

I. INTRODUCTION

Two divergent points of view have been used to describe ferromagnetism in transition metals and alloys. On one hand a localized-spin model, namely, the Heisenberg model, has been used to describe the ferromagnetism. In this model the localized spins are coupled via interatomic exchange interactions. Herring[1] has discussed at some length the objections to the pure localized spin model when applied to metals. Basically, the objections stem from the fact that the localized model fails to account for the itinerant nature of the d electrons and the nonintegral numbers of Bohr magnetons.

An itinerant-electron or band model of the Stoner–Wohlfarth type has been used to describe the ferromagnetic (FM) behavior of transition metals and alloys.[2–10] The essential features of the model as it has been applied are an exchange splitting due to an exchange interaction, treated in the molecular-field approximation (MFA), is assumed between the up- and down-spin electrons, where electron-correlation effects are taken into account using the Kanamori[11] approximation. In addition the number of itinerant electrons is assumed constant and spin-wave effects are ignored. This model is not without its objections either. Within the simplest forms of this model it is difficult to account for the rather large magnetic moments observed in some of the transition metals and alloys, and the orbital degeneracy of the d electrons and Hund's-rule effects are not generally considered.[1] However, the itinerant-electron model, based on Stoner's equations, has been used quite successfully in explaining the relationship between T_C and its initial pressure derivative $\partial T_C/\partial P$ in transition-metal alloys and compounds.[5,7,9,10,12] Furthermore, since neither Zr nor Zn is a FM metal, the ferromagnetism in $ZrZn_2$ is attributed to the itinerant electrons, where the Fermi level lies at a large peak in the density of states such that the Stoner criterion is satisfied.[3]

The recent measurements by Bartel, Edwards, and Samara[10] of T_C as a function of pressure (to high pressures) for MnSb- and Mn-substituted Invar alloys reveal some important aspects of the itinerant-electron model. Even though the results of T_C vs P to high pressure (P) in MnSb are as predicted by the itinerant-electron model, the experimental results of T_C vs P for the Invar alloys deviate markedly from the theoretical predictions of the Stoner–Wohlfarth model. For example, for the alloy $Fe_{0.65}(Ni_{0.81}Mn_{0.19})_{0.35}$, T_C decreases very nearly linearly with respect to pressure up to 32.5 kbar, whereas the calculated T_C vanishes for

P in excess of approximately 19 kbar. It was suggested that the disagreement between theory and experiment may be due to a nonconstant number of itinerant d electrons.[10] However, as shall be pointed out in this paper, the nearly linear dependence of T_C for Invar at low P and for the Mn-substituted Invar alloys to high P can be explained on the basis of a model to be discussed here.

In addition to the Stoner–Wohlfarth model, the Hubbard model[13] has been used to try to describe the ferromagnetism for itinerant electrons. However, it appears that the exact ground state, without orbital degeneracy, can never be FM.[1,14,15]

Herring[1] suggested that the model proposed by Zener[16] for the ferromagnetism in mixed-valence transition-metal oxides may be applicable to describe the ferromagnetism in transition metals. The Zener model[1,15–18] as applied to transition metals, referred to here as the modified Zener model, is described in this section. This description is essentially that given by Arai and Parrinello.[15] Consider a lattice of transition-metal atoms identical except that some have x d electrons and others have $x+1$ d electrons, where $1 \leq x \leq 4$. The same model applies when the d shell is more than half-filled, $5 \leq x \leq 8$, where d holes are treated rather than d electrons. Thus, the model is valid for cases with more than one d electron (or d hole) per atom. Furthermore, in this model it is assumed that the x electrons at each atomic site are coupled according to Hund's rule to yield the spin S of maximum multiplicity. The additional electron (Zener electron) is itinerant hopping from site to site and couples to the localized spin in accordance with Hund's rule yielding the state $S+\frac{1}{2}$ or $S-\frac{1}{2}$, depending upon the relative orientation of the two spins. Anderson and Hasegawa[19] have calculated the interaction energy for a system of two atoms sharing one itinerant electron and concluded that ferromagnetism is always favored. However, as pointed out by Arai and Parrinello,[15] the interaction energy depends on the density of Zener electrons and that in a solid an antiferromagnetic state might become stable, rather than the FM state. It should be pointed out that the model is appropriate for describing the ferromagnetism of an s-d exchange model where the d electrons produce the localized spin $\vec{S}$ and the itinerant electrons are s-like.

In this paper the primary interest will be model calculations of the dependence of T_C on the bandwidth W (or P), the effective number of itinerant d electrons per atom n, the intra-atomic exchange-interaction parameter I between the itinerant electrons of opposite spin, and the Hund's-rule-coupling-energy parameter J between the itinerant-electron spin and the localized spin. FM ordering is assumed at the outset. The model used for the calculations will be the so-called modified Zener model discussed above. In this model, the itinerant electrons are described by a Hubbard Hamiltonian and the itinerant electron couples to the localized spin (Hund's-rule coupling) by a term like $-J\vec{\sigma}\cdot\vec{S}$, where $\vec{\sigma}$ is the electron-spin operator. The itinerant electrons will be treated in the spirit of the Stoner model, i.e., in the weak-interaction limit. Major improvements of this model over the pure-itinerant-electron models are: Hund's-rule effects are taken into account, the orbital degeneracy of the d electrons is taken into account in the sense that Hund's-rule effects are taken into account, and large number of nonintegral Bohr magnetons are possible.

Of particular interest are the fcc transition-metal alloys involving Ni, Co, Fe, and Mn. The model calculations are intended to illustrate the behavior of T_C as a function of W, n, I, and J. For an actual alloy system, the effective values of I and J would be determined from the individual values for the constituent metals; for example, a coherent-potential approximation in the manner used by Harris and Zuckerman[20] can be employed to determine the effective exchange parameters. In addition, an alloy theory, possibly similar to that of Hasegawa and Kanamori,[21] should be used to determine n. Electron correlation effects as they affect the exchange energies have been omitted, but they should be included in any detailed theory for a transition metal or alloy.

The model Hamiltonian and the Green's-function (GF) solutions in the random-phase approximation (RPA) for the response functions are given in Sec. II. The GF's are of the type discussed by Zubarev.[22] Because of the inequivalent spin systems, localized and itinerant, a consequence of the model is the existence of acoustic and optic branches to the spin-wave spectrum; the spin-wave spectrum will also be discussed in Sec. II. This appearance of two spin-wave branches is identical in nature to those existing in the s-d exchange model for Pd-Fe alloys of Doniach and Wohlfarth.[23] In Sec. III the FM instability in the static long-wavelength exchange-enhanced susceptibility and the corresponding equation for T_C are determined. At T_C an effective exchange can be defined which involves both I and J. This effective exchange is calculated by considering the localized spin to interact only with the average magnetization produced by the itinerant electrons for $T \to T_C$. In addition, in Sec. III the results of model calculations, using a fcc tight-binding density of states for T_C as a function of W, n, I, and J, are discussed, as well as the consequences of the self-energy-type term. A discussion of the calculations as they relate to some experimental data is given in Sec. IV.

II. DYNAMIC SUSCEPTIBILITY AND EXCITATION SPECTRUM

In this section the model Hamiltonian will be given, and using GF techniques the response functions for the itinerant electrons and the localized spins will be calculated. In addition, the resulting excitation spectrum will be discussed. The Hamiltonian for the modified Zener model discussed in Sec. I is given by[15,17,18]

$$H=\sum_{ij\sigma}\epsilon_{ij}C_{i\sigma}^{\dagger}C_{j\sigma}+I\sum_{i}N_{i\uparrow}N_{i\downarrow}-\mu\sum_{i\sigma}N_{i\sigma}-2J\sum_{i}\vec{\sigma}_i\cdot\vec{S}_i\,, \quad (1)$$

where i and j denote the lattice sites, $C_{i\sigma}^{\dagger}$ and $C_{i\sigma}$ are the creation and annihilation operators for an electron at site i with spin $\sigma=\uparrow$ or $\downarrow$, $N_{i\sigma}=C_{i\sigma}^{\dagger}C_{i\sigma}$, and μ is the chemical potential. The energy of an electron hopping from site i to site j is ϵ_{ij}. The electrons localized on the site i interact through the intra-atomic exchange interaction I, and the Zener electron couples, according to Hund's rule, to the local spin $\vec{S}$ with an interaction parameter J. Here

$$\sigma_i^{+}=C_{i\uparrow}^{\dagger}C_{i\downarrow}\,,\quad \sigma_i^{-}=C_{i\downarrow}^{\dagger}C_{i\uparrow}\,,$$
$$\sigma_i^{z}=\tfrac{1}{2}(C_{i\uparrow}^{\dagger}C_{i\uparrow}-C_{i\downarrow}^{\dagger}C_{i\downarrow}) \quad (2)$$

are the spin operators for the electrons. The electron operators obey anticommutation relations and the spin operators obey commutation relations.

To facilitate the calculation of the dynamic susceptibility and its instability in the static long-wavelength limit, as well as calculation of the spin-wave spectrum, the Fourier-transformed operators and Hamiltonian need to be considered. The transformed operators are defined as

$$C_{i\sigma}=N^{-1/2}\sum_{k}e^{i\vec{k}\cdot\vec{i}}C_{k\sigma}\,,$$
$$C_{i\sigma}^{\dagger}=N^{-1/2}\sum_{k}e^{-i\vec{k}\cdot\vec{i}}C_{k\sigma}^{\dagger}\,, \quad (3)$$
$$\vec{S}_i=N^{-1/2}\sum_{k}e^{i\vec{k}\cdot\vec{i}}\vec{S}_k\,,$$

where N is the number of atoms per unit volume. For simplicity, k denotes $\vec{k}$ in the subscripts and $\vec{i}$ the position vector of the ith lattice site. The energy becomes

$$\epsilon_{ij}=N^{-1}\sum_{k}e^{i\vec{k}\cdot(\vec{i}-\vec{j})}\epsilon_k\,,$$
$$\epsilon_k=\sum_{\vec{i}-\vec{j}}e^{-i\vec{k}\cdot(\vec{i}-\vec{j})}\epsilon_{ij}\,. \quad (4)$$

Thus the Hamiltonian [Eq. (1)] using Eqs. (3) and (4) becomes

$$H=\sum_{k\sigma}\epsilon_k C_{k\sigma}^{\dagger}C_{k\sigma}-\mu\sum_{k\sigma}C_{k\sigma}^{\dagger}C_{k\sigma}+IN^{-1}\sum_{kk'q}C_{k+q\uparrow}^{\dagger}C_{k\uparrow}C_{k'-q\downarrow}^{\dagger}C_{k'\downarrow}$$
$$-JN^{-1/2}\sum_{kq}[C_{k+q\uparrow}^{\dagger}C_{k\downarrow}S_q^{-}+C_{k+q\downarrow}^{\dagger}C_{k\uparrow}S_q^{+}+(C_{k+q\uparrow}^{\dagger}C_{k\uparrow}-C_{k+q\downarrow}^{\dagger}C_{k\downarrow})S_q^{z}] \quad (5)$$

where, for two vectors $\vec{a}$ and $\vec{b}$,

$$\vec{a}\cdot\vec{b}=\tfrac{1}{2}(a^{+}b^{-}+a^{-}b^{+})+a^{z}b^{z}\,. \quad (6)$$

The Fourier-transformed electron operators obey the anticommutation relations

$$[C_{k\sigma},C_{k'\sigma'}^{\dagger}]_{+}=\delta_{kk'}\delta_{\sigma\sigma'}\,,$$
$$[C_{k\sigma},C_{k'\sigma'}]_{+}=[C_{k\sigma}^{\dagger},C_{k'\sigma'}^{\dagger}]_{+}=0\,, \quad (7)$$

and the Fourier-transformed spin operators obey the commutation relations

$$[S_q^{+},S_{q'}^{-}]_{-}=2N^{-1/2}S_{q+q'}^{z}\,,$$
$$[S_q^{\pm},S_{q'}^{z}]_{-}=\mp N^{-1/2}S_{q+q'}^{\pm}\,. \quad (8)$$

A. Green's-Function Equations

The thermal properties of the model Hamiltonian will be calculated using the GF techniques as discussed by Zubarev.[22] The essential equations of the GF theory for operators A and B obeying the commutation relations

$$[A,B]_{\pm}=AB\pm BA \quad (9)$$

are the Fourier-transformed equation of motion for the GF:

$$E\langle\langle A;B\rangle\rangle=(2\pi)^{-1}\langle[A,B]_{\pm}\rangle+\langle\langle[A,H]_{-};B\rangle\rangle\,, \quad (10)$$

where units of $\hbar=1$ are used. The correlation functions are calculated from

$$\langle BA\rangle=i\int_{-\infty}^{\infty}dE\,(e^{\beta E}\pm1)^{-1}(\langle\langle A;B\rangle\rangle_{E+i0}-\langle\langle A;B\rangle\rangle_{E-i0})\,, \quad (11)$$

where $\beta=1/k_BT$. The relation

$$\left(\frac{1}{E-E_k+i0}-\frac{1}{E-E_k-i0}\right)=-2\pi i\delta(E-E_k) \quad (12)$$

is also used.

B. Dynamic Susceptibility

To discuss the dynamic properties of the combined system of the localized spins coupled to the itinerant electrons, it is convenient to consider the dynamic susceptibility. The discussion given here follows closely that of Doniach and Wohlfarth[23] for the s-d exchange interaction in Pd-Fe alloys, and the work of Izuyama, Kim, and Kubo[24] on the dynamic susceptibility of an itinerant-electron system. In calculating the dynamic susceptibility the GF of interest is $\langle\langle C_{k+q\uparrow}^{\dagger}C_{k\downarrow};C_{k'+q'\downarrow}^{\dagger}C_{k'\uparrow}\rangle\rangle$, where the transverse electron-spin operators are

$$\sigma_q^+ = \sum_k C_{k+q\uparrow}^\dagger C_{k\downarrow}\,, \qquad \sigma_q^- = \sum_k C_{k+q\downarrow}^\dagger C_{k\uparrow}\,. \tag{13}$$

Thus, the transverse electron-spin GF is

$$K(\vec{q}, E) \equiv \langle\langle \sigma_q^+ ; \sigma_{-q}^- \rangle\rangle = N^{-1} \sum_{kk'} \langle\langle C_{k+q\uparrow}^\dagger C_{k\downarrow} ; C_{k'-q\downarrow}^\dagger C_{k'\uparrow} \rangle\rangle\,, \tag{14}$$

where the GF's involved are calculated using Eq. (10). The resulting higher-order GF's are to be decoupled in the RPA. The essential strategy of the RPA decoupling scheme is to factor the thermal averages of operators which are nonzero in first order; these thermal averages are the electron-number operators $n_{k\sigma} \equiv \langle C_{k\sigma}^\dagger C_{k\sigma} \rangle$ and the average localized spin per site $\bar{S} \equiv \langle S^z \rangle$ which is assumed to be the same for all sites.

In calculating the GF given by Eq. (14), the procedures used by Doniach and Wohlfarth[23] and Izuyama *et al.*[24] will be employed except the GF's used here are defined differently than in the previous work (Refs. 23 and 24). Therefore, for the sake of brevity only the final results will be given. The electron magnetization $n\zeta$ is defined as

$$n\zeta = N^{-1} \sum_k (n_{k\uparrow} - n_{k\downarrow}) \tag{15}$$

and n, the number of itinerant d electrons per atom, is defined as

$$n = N^{-1} \sum_k (n_{k\uparrow} + n_{k\downarrow})\,, \tag{16}$$

where ζ is the magnetization per electron. Thus, from Eqs. (15) and (16),

$$n_\uparrow = \tfrac{1}{2}(n + n\zeta)\,, \quad n_\downarrow = \tfrac{1}{2}(n - n\zeta)\,, \tag{17}$$

where $n_\sigma = N^{-1}\sum_k n_{k\sigma}$. The resultant GF $K(\vec{q}, E)$ is[23]

$$K(\vec{q}, E) = \frac{-(2\pi)^{-1}\chi^0(\vec{q}, E)}{1 - [I - 2J^2\bar{S}/(E - Jn\zeta)]\,\chi^0(\vec{q}, E)}\,, \tag{18}$$

where the unenhanced susceptibility $\chi^0(\vec{q}, E)$ is given by

$$\chi^0(\vec{q}, E) = -N^{-1} \sum_k \frac{n_{k+q\uparrow} - n_{k\downarrow}}{E - (\epsilon_k - \epsilon_{k+q}) - \Delta}\,, \tag{19}$$

and where

$$\Delta = In\zeta + 2J\bar{S} \tag{20}$$

is the Stoner splitting.

The response function has been defined in terms of retarded GF by Zubarev.[22] Therefore, the real part of a *reduced* transverse (or perpendicular) susceptibility is defined as[22,25]

$$\chi(\vec{q}, E) = -2\pi K(\vec{q}, E)\,, \tag{21}$$

where the response function is defined as transverse (perpendicular) to the applied field and not transverse to $\vec{q}$. The susceptibility defined by Eq. (21) is the so-called isolated susceptibility. It has been shown that the long-wavelength static isolated susceptibility is bounded from above by the adiabatic susceptibility which in turn is bounded from above by the isothermal susceptibility.[26,27] In what follows, the word "isolated" will be suppressed when referring to the reduced susceptibility defined by Eq. (21).

The transverse GF for the localized spins of interest is $\langle\langle S_q^+ ; S_{-q}^- \rangle\rangle$, from which the transverse correlation function can be calculated. Following the procedures and decoupling scheme outlined above,

$$\langle\langle S_q^+ ; S_{-q}^- \rangle\rangle = \frac{(2\pi)^{-1} 2\bar{S}}{E - Jn\zeta + 2J^2\bar{S}\,\chi^0(\vec{q}, E)\,[1 - I\chi^0(\vec{q}, E)]^{-1}}\,, \tag{22}$$

where the Fourier transform of $\langle\langle S_q^+ ; S_{-q}^- \rangle\rangle$ is defined as

$$\langle\langle S_i^+ ; S_j^- \rangle\rangle = N^{-1} \sum_q e^{i\vec{q}\cdot(\vec{i} - \vec{j})}\, \langle\langle S_q^+ ; S_{-q}^- \rangle\rangle\,. \tag{23}$$

C. Single-Particle Excitations

The itinerant-electron magnetization $n\zeta$ and the electron thermal averages $n_{k+q\uparrow} - n_{k\downarrow}$ appear in the expressions for $K(\vec{q}, E)$, $\langle\langle S_q^+ ; S_{-q}^- \rangle\rangle$, and $\chi^0(\vec{q}, E)$. The electron thermal averages are calculated from the single-particle GF $\langle\langle C_{k\sigma} ; C_{k\sigma}^\dagger \rangle\rangle$. Using Eqs. (5), (7), (10), and the RPA decoupling procedure, the GF becomes

$$\langle\langle C_{k\sigma} ; C_{k\sigma}^\dagger \rangle\rangle = (2\pi)^{-1}/(E - \epsilon_{k\sigma})\,, \tag{24}$$

where

$$\epsilon_{k\pm} = \epsilon_k - \epsilon_F \mp \tfrac{1}{2}In\zeta \mp J\bar{S}\,, \quad -\text{for } \sigma = \uparrow,\ +\text{for } \sigma = \downarrow \tag{25}$$

and

$$\epsilon_F = \mu - \tfrac{1}{2}In\,. \tag{26}$$

Here $\bar{\sigma}$ will denote the spin direction opposite to that of σ. Note that the single-particle excitation energy [Eq. (25)] is similar to the Hartree–Fock result where the electron of spin σ interacts with the average field of the $\bar{\sigma}$ electrons; plus, in this case, the electrons interact with the average localized-spin magnetization. Thus, the energy difference between the up- and down-spin electrons is the Stoner splitting [Eq. (20)]. From Eqs. (11), (12), and (24) the thermal average of the number operator becomes

$$n_{k\sigma} \equiv \langle C_{k\sigma}^\dagger C_{k\sigma} \rangle = (e^{\beta\epsilon_{k\sigma}} + 1)^{-1} \equiv f(\epsilon_{k\sigma})\,, \tag{27}$$

where $f(x)$ is the Fermi distribution function.

D. Physical Picture

For the approximations used in the above calculations, the physical model for the interaction of the itinerant electron with the localized-spin system is as follows. As explained above, the single-particle energies, [Eq. (25)], are calculated in the spirit of the Hartree–Fock approximation in that

an electron of a given spin polarization interacts with the average field created by the electrons of the opposite spin polarization; in addition, the electrons interact with the average spin polarization of the localized spins. For the itinerant-electron spin operators [Eq. (13)] the electron spin interacts with the average magnetization produced by the itinerant electrons $n\zeta$ and the localized spin $\bar{S}$; in addition, certain electron correlations are taken into account.[24] According to Wolff,[28] these correlations correspond to certain ladder diagrams; however, as he pointed out, these diagrams do not account for all electron correlation effects. In this case, account is taken of fluctuations in the average $n\zeta$ and $\bar{S}$. For the localized-spin operators [Eq. (22)] the localized spin interacts primarily with $n\zeta$, the $Jn\zeta$ term in Eq. (22), plus a term proportional to $\bar{S}$. The real part of this term proportional to $\bar{S}$ gives a level shift to $Jn\zeta$ and the imaginary part gives rise to a damping. This level shift and damping come from the fluctuations in $n\zeta$ through $\chi^0(\vec{q}, E)$.

E. Spin-Wave Spectrum

The excitation energies for the electron and localized spins are found from the zeros in the denominators of $K(\vec{q}, E)$ and $\langle\langle S_q^+; S_{-q}^- \rangle\rangle$ which yield identical energy spectra. Following Izuyama *et al.*[24] and Doniach and Wohlfarth,[23] the excitation energies for small $\vec{q}$ become

$$\begin{aligned} E(\mathrm{ac})_q &= Dq^2 \quad \text{(acoustic branch)}, \\ E(\mathrm{op})_q &= E_{\mathrm{op}} + D(IE_{\mathrm{op}}/J\Delta - 1)q^2 \quad \text{(optic branch)}, \end{aligned} \tag{28}$$

where the coefficient D can be determined from Refs. 23 and 24 and E_{op} is

$$E_{\mathrm{op}} = Jn\zeta + 2J\bar{S} \ . \tag{29}$$

Since there are two inequivalent spin systems, the itinerant electrons and localized spins, there are two branches to the spin-wave spectrum, an acoustic and an optic branch. In addition, there are the so-called Stoner excitations, which are found from the singularities in $\chi^0(\vec{q}, E)$—these singularities give rise to a continuum of excitation energies, i.e., branch cuts.

The resulting excitation spectrum is illustrated schematically in Fig. 1. In the spectrum are illustrated the acoustic and optic spin-wave branches and the Stoner excitations where in Fig. 1 it is assumed that $J < I$. The dashed portions of the spin-wave branches illustrate that when these energies approach the Stoner energies, the elementary excitations are not well-defined excitations and are damped due to the Stoner excitations.

Experimentally, the acoustic branch has been observed and measured in some transition metals and alloys.[29] However, as far as this author is aware, the optic branch has not been observed in transition metals and alloys. The reason for this may be that E_{op} is probably on the order of 0.1–0.5 eV (above the neutron energies usually used) or if $J \sim I$ the optic-branch energy is not well defined because of the Stoner excitations. Investigation of this optic branch would be important in verifying if this model is appropriate for the description of ferromagnetism in transition metals and alloys.

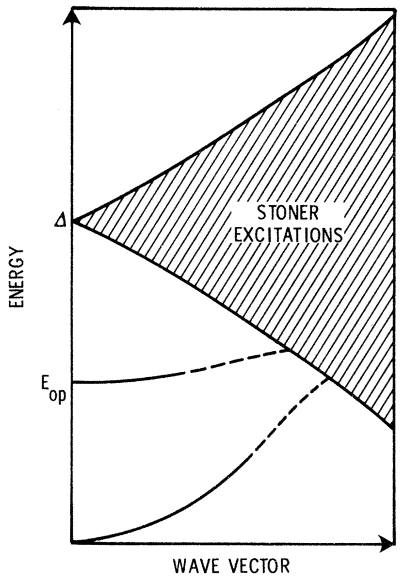

FIG. 1. Schematic drawing of the excitation spectrum for the modified Zener model. Shown are the acoustic and optic spin-wave branches and the continuum Stoner excitations. The dashed portions of the curves indicated that the excitations are not well defined. Here Δ is the Stoner splitting defined by Eq. (20), E_{op} is the $\vec{q}=0$ optic-branch energy defined by Eq. (29), and it is assumed in the figure that $I > J$.

III. CALCULATIONS OF T_C

The FM instability is found from the singularity in the $\vec{q} \to 0$, $E \to 0$, $\Delta \to 0$ limit of the exchanged-enhanced susceptibility $\chi(\vec{q}, E)$ given by Eqs. (18) and (21). The temperature at which this instability occurs is called the Curie temperature T_C. Taking the above limit requires taking the $\vec{q} \to 0$, $E \to 0$, $\Delta \to 0$ limit of the unenhanced susceptibility $\chi^0(\vec{q}, E)$ as defined by Eq. (19). This is accomplished by taking the limit of $\vec{q} \to 0$ and $E \to 0$ and then $\Delta \to 0$. In the limit $\Delta \to 0$, $n_{k\uparrow} = n_{k\downarrow}$. Thus, from Eqs. (19) and (27) in the limit of $\Delta \to 0$ for $T \to T_C$ and using a Taylor's series expansion of $f(\epsilon_k)$, $\chi^0(0, 0)$ becomes

$$\chi^0(0, 0)\big|_{\Delta \to 0} = -N^{-1} \sum_k \frac{\partial f(\epsilon_k)}{\partial \epsilon_k}\bigg|_{T_C} , \tag{30}$$

where $f(\epsilon_k)$ is defined by Eq. (27). Replacing the summation in Eq. (30) with an integral over the

density of states per atom per spin direction, $N(\epsilon)$, and defining $\chi^0(0,0)_{\Delta\to 0}\equiv\bar{\chi}^0(T_C)$, Eq. (30) becomes

$$\bar{\chi}^0(T_C)=\int d\epsilon\, N(\epsilon)\left|\frac{\partial f(\epsilon)}{\partial\epsilon}\right|_{T_C}, \tag{31}$$

where ϵ now denotes the energy E.

Therefore, from Eqs. (18) and (30) or (31), the singularity in the exchange-enhanced susceptibility occurs when

$$I_{\rm eff}\bar{\chi}^0(T_C)=1, \tag{32}$$

where

$$I_{\rm eff}\equiv\left(I+\frac{2J\bar{S}}{n\zeta}\bigg|_{n\zeta\to 0}\right). \tag{33}$$

Note that the evaluation of $n\zeta=n_\uparrow-n_\downarrow$ [Eq. (15)] for a Stoner splitting [Eq. (20)] between "up" and "down" spins in the limit of $\Delta\to 0$ at $T=T_C$ yields the same result as given by Eq. (32) for the FM instability. As is evident from its definition, $\bar{\chi}^0(T_C)$ depends on the value of ϵ_F, which in turn depends on the temperature T_C, where the value of n determines ϵ_F. Thus, in order to solve for T_C when the limit $(\bar{S}/n\zeta)_{n\zeta\to 0}$ is evaluated, it is necessary to solve the expression for n obtained from Eq. (16) with $\Delta=0$,

$$n=2\int d\epsilon\, N(\epsilon)f(\epsilon), \tag{34}$$

and Eq. (32) in a simultaneous self-consistent manner for T_C and ϵ_F.[30]

A. Evaluation of $(S/n\zeta)_{n\zeta\to 0}$ in the Mean-Field Approximation

Using what are now more-or-less standard techniques, $\bar{S}$ as a function of T can be calculated. In this work, the procedure used by Lines[31] for an antiferromagnetic system (it also applies to a ferromagnetic system) will be employed. Thus, for a spin S, $\bar{S}$ can be found from[31]

$$\frac{2\bar{S}+y}{2S+1}=\frac{(y+1)^{2S+1}+(y-1)^{2S+1}}{(y+1)^{2S+1}-(y-1)^{2S+1}}, \tag{35}$$

where here

$$y=1+\langle S_i^- S_i^+\rangle/\bar{S}. \tag{36}$$

In the limit of $T\to T_C$, $y\to\infty$ such that $\bar{S}\to 0$. Expanding Eq. (35) for large y, the solution for $\bar{S}$ is

$$\bar{S}=\tfrac{2}{3}S(S+1)\,y^{-1},\quad T\to T_C. \tag{37}$$

The correlation function $\langle S_i^- S_i^+\rangle$ is calculated from the GF, $\langle\langle S_i^+;\, S_i^-\rangle\rangle$. This GF can be calculated from Eqs. (1) and (10). The mean-field-approximation result for this GF is to keep only those terms which when decoupled are nonzero in first order, i.e., either the thermal average of the term decoupled or the GF are to be nonzero in first order. In this case, the resultant term which is kept is the interaction of the localized spin with the average magnetization produced by the itinerant electrons and the GF becomes

$$\langle\langle S_i^+;\, S_i^-\rangle\rangle=\frac{(2\pi)^{-1}2\bar{S}}{E-Jn\zeta}. \tag{38}$$

Using Eqs. (11), (12), and (38) the correlation function of interest in this approximation becomes

$$\langle S_i^- S_i^+\rangle=2\bar{S}(e^{\beta Jn\zeta}-1)^{-1}, \tag{39}$$

and thus

$$y=\coth\tfrac{1}{2}\beta Jn\zeta. \tag{40}$$

Note that the mean-field result for the GF [Eq. (38)] could be obtained from the GF given by Eqs. (22) and (23) when the last term in the denominator of Eq. (22) is neglected. Neglecting this term is equivalent to neglecting spin-wave effects. The omission of this term will be discussed in Sec. III D. In the limit of $T\to T_C$, $y\to 2k_BT_C/Jn\zeta$ so from Eq. (37), $(\bar{S}/n\zeta)_{n\zeta\to 0}$ becomes

$$\frac{\bar{S}}{n\zeta}\bigg|_{n\zeta\to 0}=\frac{1}{3}\,\frac{S(S+1)J}{k_BT_C}. \tag{41}$$

Thus, from Eqs. (33) and (41), $I_{\rm eff}$ becomes

$$I_{\rm eff}=I+2S(S+1)J^2/3k_BT_C \tag{42}$$

for this approximation.

From Eqs. (39) and (41) the correlation function for $T=T_C$ becomes

$$\langle S_i^- S_i^+\rangle|_{T_C}=\tfrac{2}{3}S(S+1) \tag{43}$$

in agreement with results for localized spins using a Heisenberg model; see, e.g., Ref. 31. This agreement leads one to conclude that the above approximation is reasonable.

B. Density of States

In this paper a tight-binding density of states $N(\epsilon)$ for an fcc lattice will be used in Eq. (31). For $N(\epsilon)$ the nearest-neighbor (nn) and next-nearest-neighbor (nnn) interactions will be considered. The tight-binding energies for the fcc lattice are found from Eq. (4). Using Heine's[32] results for the dependence of the d bandwidth on interatomic distance R,

$$\frac{\partial\ln W}{\partial\ln R}=-5, \tag{44}$$

the ratio of the nn to nnn interactions can be calculated and the resultant tight-binding energy is

$$\begin{aligned}\epsilon_k=4\epsilon_0[&(\cos\tfrac{1}{2}k_xa\cos\tfrac{1}{2}k_ya\\&+\cos\tfrac{1}{2}k_ya\cos\tfrac{1}{2}k_za+\cos\tfrac{1}{2}k_xa\cos\tfrac{1}{2}k_za)\\&+2^{-7/2}(\cos k_xa+\cos k_ya+\cos k_za)],\end{aligned} \tag{45}$$

where ϵ_0 is the nn transfer-energy parameter and a the lattice spacing. The density of states per atom per spin direction $N(\epsilon)$ is calculated using[33]

$$N(\epsilon)=N^{-1}\sum_k\delta(\epsilon-\epsilon_k). \tag{46}$$

Then using this $N(\epsilon)$ in Eqs. (31) and (34), T_C as a function of ϵ_0, I, J, and n can be calculated, where I_{eff} is the mean-field-approximation value given by Eq. (42).

C. Calculations

The numerical computations were carried out in the following manner. In the calculations of $N(\epsilon)$ from Eq. (46) using the ϵ_k given by Eq. (45), the bandwidth was divided into 100 equal segments and the number of states falling into each energy interval tabulated. For an fcc lattice the second Brillouin zone is simple cubic, thus for the ease of the summation in Eq. (46), the summation was carried out over one octant of the first two zones with the proper normalization. Thus, in Eq. (45), $0 \leq k_i a \leq 2\pi$, where i denotes x, y, or z. In calculating the integration in $\bar{\chi}^0(T_C)$, Eq. (31), and for n, Eq. (34), a polynomial of order 20 was fit to the tabulated values of $N(\epsilon)$. The integrated area for the polynomial expression for $N(\epsilon)$ was within 0.4% of that for the tabulated $N(\epsilon)$, even though the agreement at any one point was not, in general, that good. The result for the polynomial expression for $N(\epsilon)$ with $\epsilon_0 = -0.2$ eV is shown in Fig. 2. In using the polynomial expression for $N(\epsilon)$, sharp peaks arising from $|\partial f/\partial\epsilon|$ in $\bar{\chi}^0(T_C)$, which are narrower than the step size in the tabulated $N(\epsilon)$, are properly taken into account. The simultaneous self-consistent solutions for n and T_C were solved to within ± 0.001 and 1 °K, respectively.

When the itinerant-electron spins are aligned antiferromagnetically with respect to the localized spins, i.e., $\vec{\sigma}_i \cdot \vec{S}_i < 0$ in Eq. (1), this case would be equivalent to putting $J < 0$ in the work of this paper. The instability for this type of ordering occurs when Eq. (32) is satisfied; I_{eff} [Eq. (42)] is independent of the sign of J and the calculations given here for T_C as a function of W, n, J, and I are applicable to this type of ordering.

Calculations of T_C as functions of W, n, I, and J are shown in Figs. 3–7. The parameters were chosen so as to give values of T_C more or less in agreement with experimental values for the fcc transition-metal alloys. These model calculations are intended to illustrate the behavior of T_C for various W, n, I, and J. As pointed out in Sec. I, a detailed alloy theory for the effective values of I, J, S, and n is needed before a detailed comparison of theory and experiment can be made for the transition-metal-alloy systems.

The model calculations of T_C with $J = 0$ correspond to a pure itinerant-electron ferromagnet of the Stoner–Wohlfarth type where there is no coupling to a localized spin. A FM state can exist if the Stoner criterion (SC) $I_{\text{eff}} N(\epsilon_F) > 1$ (at $T = 0$) is satisfied (for $J = 0$, $I_{\text{eff}} = I$). Calculations of $N(\epsilon)$ as a function of W show that $N(\epsilon_F)$ scales as W^{-1}. In Fig. 3 are shown results of calculations of T_C vs n for various J's with $S = 1$, $I = 0.90$ eV, and $W = 3.42$ eV; n represents the number of electrons and the number of holes is given by $2 - n$, where the nondegenerate d band is capable of holding two electrons, one for each spin direction. Here n was chosen such that ϵ_F is near the peak in $N(\epsilon)$, and Fig. 2 shows the relative positions of ϵ_F for $n = 1.2$, 1.4, 1.6, and 1.8 at $T = 0$. From Fig. 3 it is apparent that the existence of the FM state

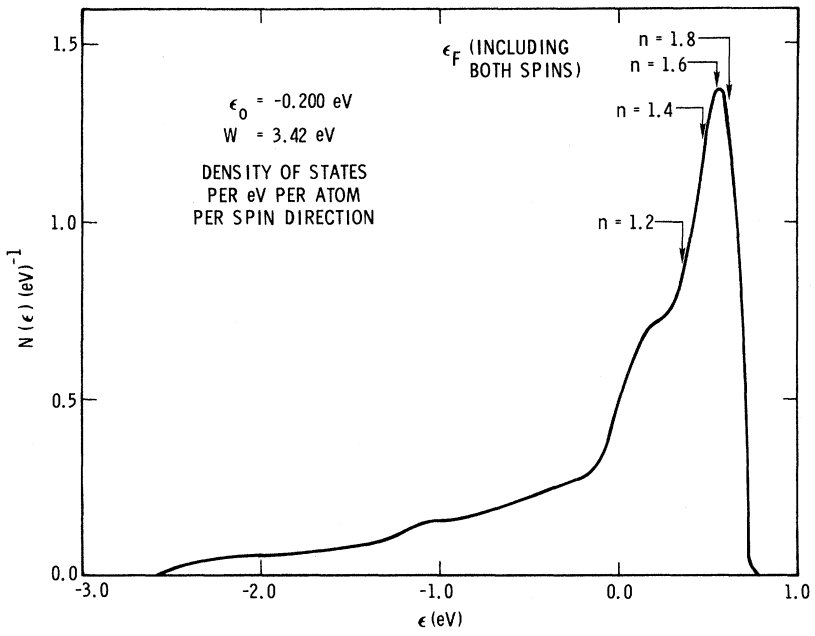

FIG. 2. Calculated density of states per eV per atom per spin direction for a fcc lattice in the tight-binding approximation including nn and nnn interactions. In the calculations the nn transfer energy ϵ_0 is assumed to be $\epsilon_0 = -0.2$ eV giving a bandwidth of $W = 3.42$ eV. The relative positions of ϵ_F for various n's are shown where the indicated n's are for the number of electrons for both spin directions.

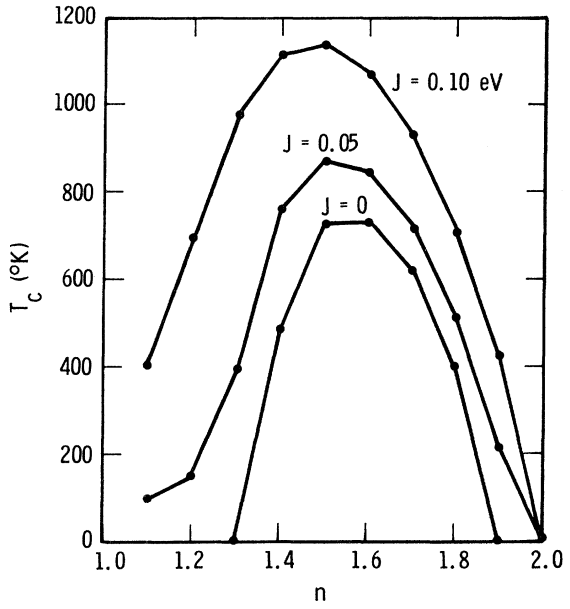

FIG. 3. Calculations of T_C as a function of n for various J's. The solid circles are calculated values and the solid connecting straight lines are shown for clarity. In the calculations $S=1$, $I=0.90$ eV, and $W=3.42$ eV.

depends quite strongly on n. This dependence arises because for $n \cong 1.9$ or $n \lesssim 1.3$, $N(\epsilon_F)$ is small and for a small J [Eq. (32)], i.e., the SC cannot be satisfied. For the larger values of J, I_{eff} [Eq. (42)] becomes large for small values of T_C, and thus ferromagnetism can occur because the SC can be satisfied. In Fig. 4 are shown results of calculations of T_C vs I for various n and J with $S=1$ and $W=3.42$ eV; thus combining the results shown in Figs. 3 and 4, T_C vs n for various I's can be determined.

In Figs. 5–7 are shown results of model calculations of T_C vs W for various n and J with $S=1$. Note that W and the pressure P are related through Eq. (44) so the figures represent calculations of T_C vs P. When the SC is satisfied for the range of parameters used for $J=0$, note the quadraticlike vanishing of T_C for an increasing W. This behavior, as expected, is in agreement with the predictions of the Stoner–Wohlfarth model.[10] For $J \neq 0$, T_C as a function of W can take on a quadraticlike behavior when $T_C \gg 0$, a concave upwards behavior when $T_C \to 0$, or a nearly linear behavior depending upon the value of J as well as the values of the other parameters. Also in Figs. 5–7 are shown curves for which $IN(\epsilon_F) < 1$ and the FM state exist by virtue of the itinerant-electron-localized spin coupling, i.e., for $J \neq 0$ the condition $I_{\text{eff}} N(\epsilon_F) \geq 1$ is satisfied even though $IN(\epsilon_F) < 1$. In this case the concave upwards behavior of T_C vs W is due to the T_C^{-1} term in I_{eff} given by Eq. (42).

The effective exchange I_{eff} for $J \neq 0$ gets larger as $T_C \to 0$. However, for W quite large, $N(\epsilon_F)$ is small such that the condition $I_{\text{eff}} N(\epsilon_F) < 1$ can exist except at $T_C = 0$, where $I_{\text{eff}} \to \infty$ in this approximation. For the T_C-vs-W curves with $J = 0.01$ eV the FM state vanishes (at least $T_C < 0.8$ °K) as illustrated in Figs. 5–7. As will be shown in Sec. III D, the effect of the self-energy-type term is that I_{eff} does not diverge as $T_C \to 0$ but has some finite value.

D. Discussion of the Self-Energy Term

In the mean-field approximation discussed in Sec. III A, I_{eff} diverges as $T_C \to 0$. The purpose of the following discussion is to show that within a constant-level shift-constant damping approximation, the self-energy-type term in the denominator of Eq. (22) keeps $(\bar{S}/n\zeta)_{n\zeta \to 0}$ from diverging in the limit $T_C \to 0$. The approximation to be used was motivated by Anderson's[34] work on the localized states in metals for an isolated impurity. In his work the approximation of the wave-vector independence of the virtual-level width is quite reasonable for an isolated impurity; whereas here for an extended system, this type of an approximation needs further explanation.

From Eqs. (12) and (19) the unenhanced susceptibility can be written

$$\chi^0(\vec{q}, E \pm i0) = \chi^0(\vec{q}, E)' \pm i\chi^0(\vec{q}, E)'' , \tag{47}$$

where

$$\chi^0(\vec{q}, E)' = -\frac{P}{N} \sum_k \frac{n_{k+q} - n_k}{E - (\epsilon_k - \epsilon_{k+q}) - \Delta} ,$$

$$\chi^0(\vec{q}, E)'' = \pi N^{-1} \sum_k (n_{k+q} - n_k) \times \delta(E - (\epsilon_k - \epsilon_{k+q}) - \Delta) \tag{48}$$

for the real and imaginary parts of $\chi^0(\vec{q}, E)$, and where P denotes the principal part of the sum. The last term in the denominator of Eq. (22), the self-energy term, can be written in the form $\Sigma(\vec{q}, E \pm i0) = \Sigma'(\vec{q}, E) \pm i\Sigma''(\vec{q}, E)$. The calculation of $\langle S_i^- S_i^+ \rangle$, needed to calculate $\bar{S}$, involves a summation over $\vec{q}$ and an integration over E. Now assuming that if Σ' and/or Σ'' are discontinuous that they can be approximated by continuous functions, then one is in a position to apply the mean-value theorem for integrals to the $\vec{q}$ summation and the E integration. Instead of applying the theorem directly, it is assumed that constants λ and Γ exist such that the spin GF, Eq. (22), is given approximately by

$$\langle\langle S_q^+ ; S_{-q}^- \rangle\rangle_{E \pm i0} \cong \frac{(2\pi)^{-1} 2\bar{S}}{E - Jn\zeta + \lambda\bar{S} \pm i\Gamma(E)\bar{S}} , \tag{49}$$

$$\Gamma(E) = \begin{cases} \Gamma, & \Delta - \bar{W} \leq E \leq \Delta + \bar{W} \\ 0, & \text{otherwise} \end{cases} \tag{50}$$

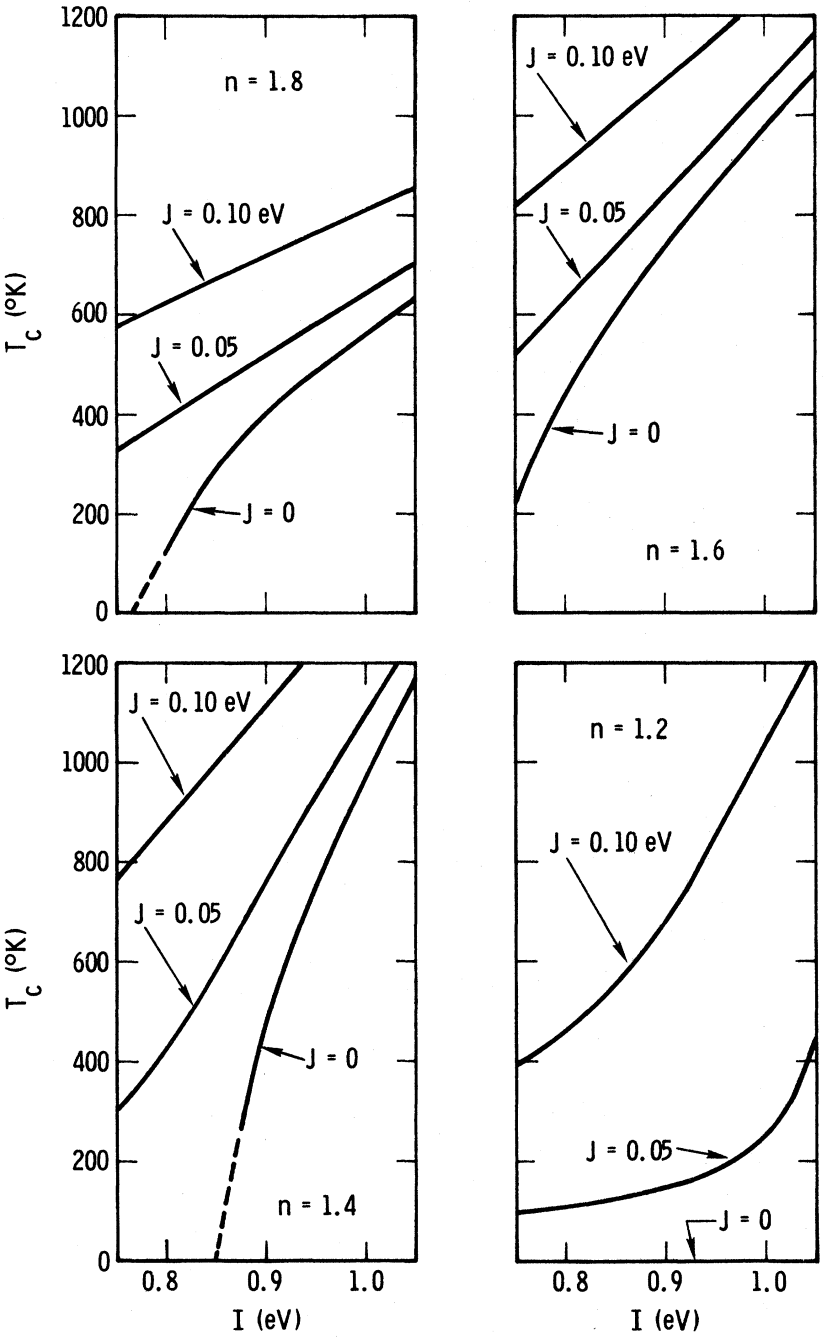

FIG. 4. Calculation of T_C as a function of I for various J's and n's with $S=1$ and $W=3.42$ eV. The dashed portions of the curve indicate extrapolations of the calculated curves. For $n=1.8$ and $J=0$, the FM state vanishes for $I \lesssim 0.75$ eV, and for $n=1.4$, and $J=0$, the FM state vanishes for $I \lesssim 0.85$ eV.

where $\overline{W}$ is an effective bandwidth consistent with the energies defined by Eq. (4) and the Fermi factors in Eq. (48); thus, $\overline{W} \sim \epsilon_F$. In this work the constants λ and Γ are considered to be proportional to the energy and wave-vector averages of $\Sigma'(\vec{q}, E)$ and $\Sigma''(\vec{q}, E)$ such that Eq. (49) is approximately true. Note that if one assumes that one can approximate the GF, $\langle\langle S_q^+; S_{-q}^- \rangle\rangle$, by evaluating Σ' and Σ'' at E and $\vec{q}$, which give the maximum contribution to the GF, then the GF is of the form given by Eq. (49). The exact form of Eq. (49) has not been proven; however, from the above arguments it does seem justified for the purposes of this discussion.

From Eqs. (11) and (49)

$$\langle S_i^- S_i^+ \rangle = \frac{2\overline{S}}{2\pi} \int_{\Delta - \overline{W}}^{\Delta + \overline{W}} \frac{dE}{e^{\beta E} - 1} \times \left(\frac{2\Gamma\overline{S}}{(E - Jn\zeta + \lambda\overline{S})^2 + \Gamma^2\overline{S}^2} \right) . \quad (51)$$

In the limit $\Delta \to 0$ and $\bar{W} \gg J$, Eq. (51) becomes

$$\langle S_i^- S_i^+ \rangle \to \frac{2\bar{S}}{\exp[\beta(Jn\zeta - \lambda\bar{S} + i\Gamma\bar{S})] - 1} \quad . \tag{52}$$

In the limit $\Gamma\bar{S} \to 0$, from Eqs. (36), (37), and (52), $(\bar{S}/n\zeta)_{n\zeta \to 0}$ in this approximation becomes

$$\left.\frac{\bar{S}}{n\zeta}\right|_{n\zeta \to 0} = \frac{S(S+1)J}{3k_B T_C + \lambda S(S+1)} \quad , \tag{53}$$

and I_{eff} [Eq. (33)] becomes

$$I_{\text{eff}} = I + \frac{2S(S+1)J^2}{3k_B T_C + \lambda S(S+1)} \quad . \tag{54}$$

In the limit $\Gamma\bar{S} \to 0$, $\langle S_i^- S_i^+ \rangle$ from Eqs. (52) and (53) is just the Heisenberg-model value for the correlation function at $T = T_C$ as given by Eq. (43); thus, the above approximation seems reasonable.

The purpose of discussing the inclusion of the $\Sigma(\vec{q}, E)$ term within the above approximation is to show that the contribution of this term keeps $(\bar{S}/n\zeta)_{n\zeta \to 0}$ from diverging in the limit $T_C \to 0$. Even though the approximation used is quite crude, it is felt that the essential feature of this approximation, namely, the fact that $(\bar{S}/n\zeta)_{n\zeta \to 0}$ does not diverge for $T_C \to 0$, is the same as would be obtained from a substantially more elaborate approximation or a numerical treatment.

Crude estimates of λ yield the result that λ is probably quite small for small J, and this term only becomes important in the limit $T_C \to 0$. In the limit $3k_B T_C \ll \lambda S(S+1)$, I_{eff} becomes independent of T_C and the behavior of T_C vs W would be similar to that of a pure itinerant model with a quadraticlike behavior when $T_C \to 0$. Therefore, it is clear that

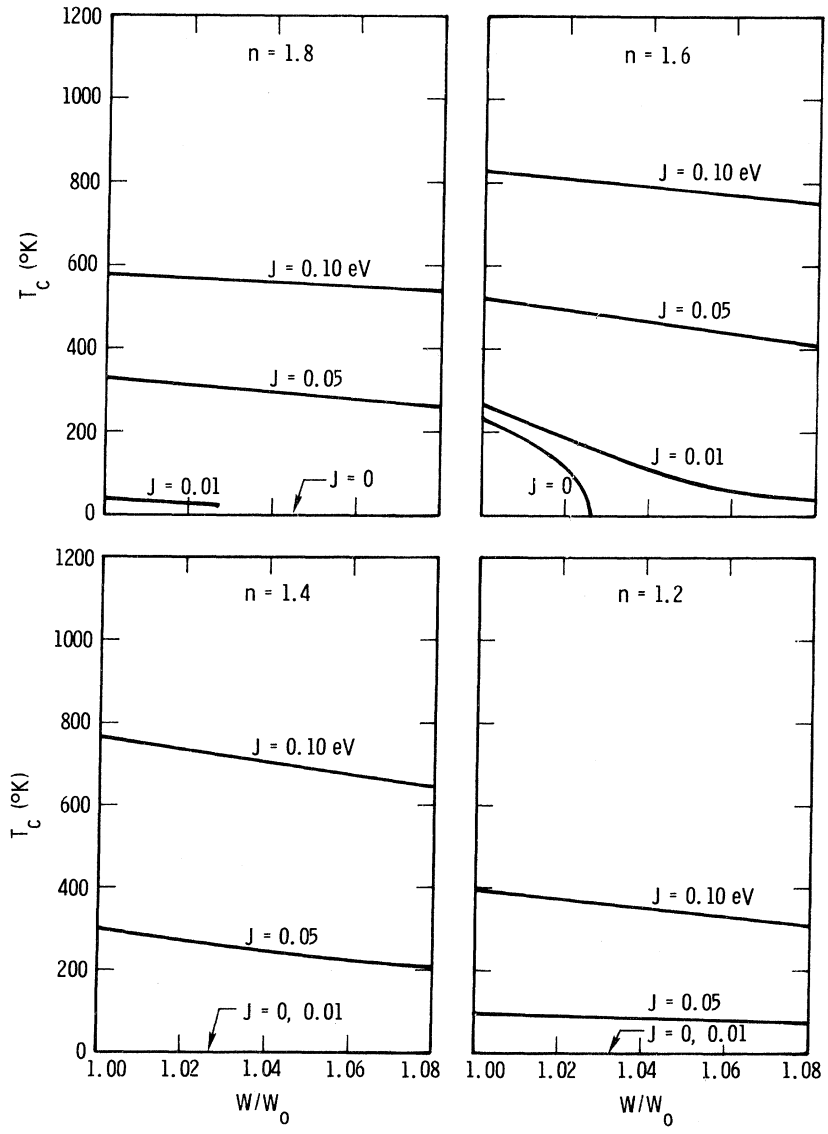

FIG. 5. Calculations of T_C as a function of W/W_0 for various J's and n's with $S = 1$, $W_0 = 3.42$ eV, and $I = 0.75$ eV. For $n = 1.8$, and $J = 0.01$ eV, the FM state vanishes for $1.0275 < W/W_0 < 1.03$. The concave upwards appearance of the $n = 1.6$, $J = 0.01$-eV curve is due to the T_C^{-1} term in I_{eff}.

the mean-field approximation for I_{eff}, Eq. (42), is not valid at extremely low temperatures, and at these low temperatures one must include the self-energy-type term $\Sigma(\vec{q}, E)$.

IV. DISCUSSION

Penn's[35] calculations for a pure-itinerant ferromagnet indicate that for a half-filled band, $n=1$, the ordering is antiferromagnetic. When $n<1$ or $n>1$ the ordering is FM.[35] For the modified Zener model discussed in this paper, the itinerant electrons align the localized spins; thus if the itinerant electrons ferromagnetically (antiferromagnetically) order, then one expects the localized spins to ferromagnetically (antiferromagnetically) order. In this paper the antiferromagnetic order for the half-filled band has not been investigated.

The model calculations reported on here predict behavior of T_C vs W and T_C vs n, which are in general agreement with experimental observations in transition-metal alloys. Leger and Susse-Loriers[36] observed a quadraticlike dependence of T_C vs P in Invar ($Fe_{0.65}Ni_{0.35}$) to high pressure, $T_C = 260$ °K at $P = 54$ kbar. For $Fe_{0.70}Ni_{0.30}$ they observed that T_C depends linearly on P to $P = 52$ kbar. In addition for Invar and some Mn-substituted Invar alloys[10] $[Fe_{0.65}(Ni_{1-x}Mn_x)_{0.35}$ for $0 \le x \le 0.19]$, it was observed that T_C decreases linearly with increasing P for $P \le 20$ kbar ($x=0$), $P \le 20$ kbar ($x=0.09$), $P \le 30$ kbar ($x=0.16$), and $P \le 32.5$ kbar ($x=0.19$). The linear and quadraticlike behavior is consistent with the T_C-vs-W calculations shown in Figs. 5–7. A 1% change in W corresponds to a pressure of approximately 11 kbar. The quadraticlike behavior

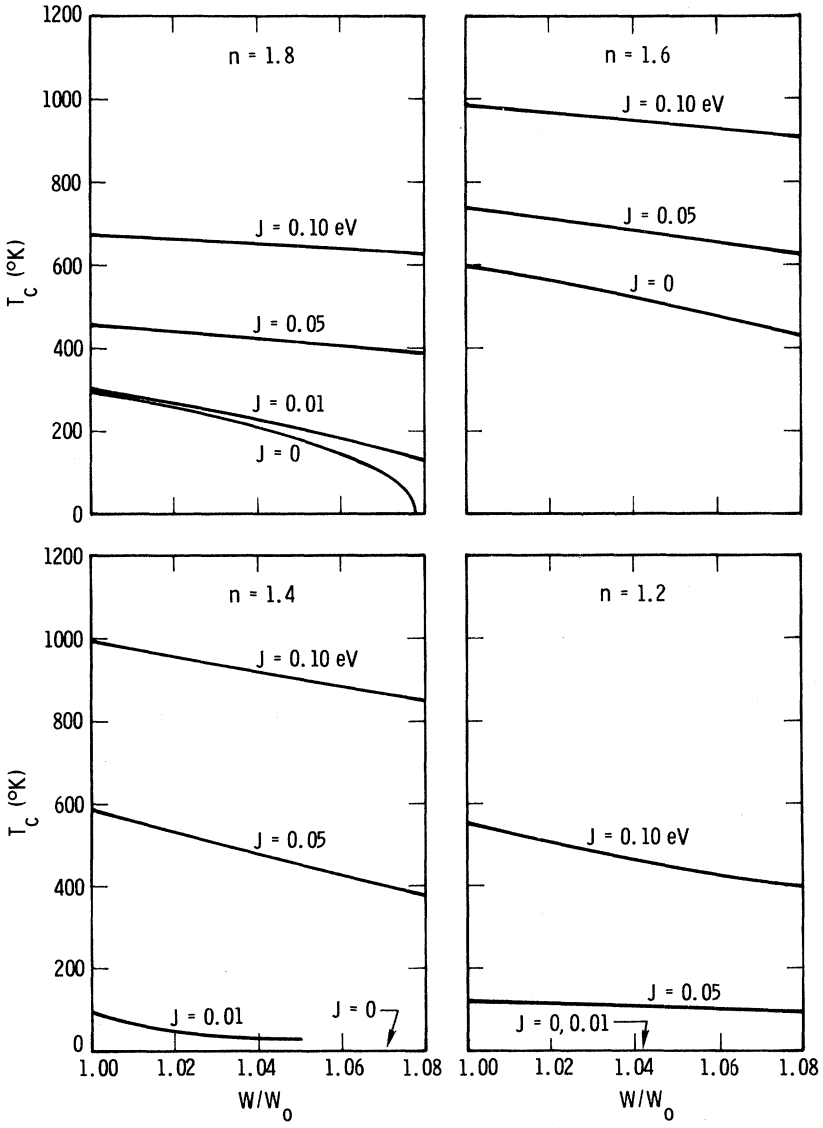

FIG. 6. Calculations of T_C as a function of W/W_0 for various J's and n's with $S=1$, $W_0=3.42$ eV, and $I=0.85$ eV. For $n=1.4$ and $J=0.01$ eV, the FM state vanishes for $1.05 < W/W_0 < 1.055$.

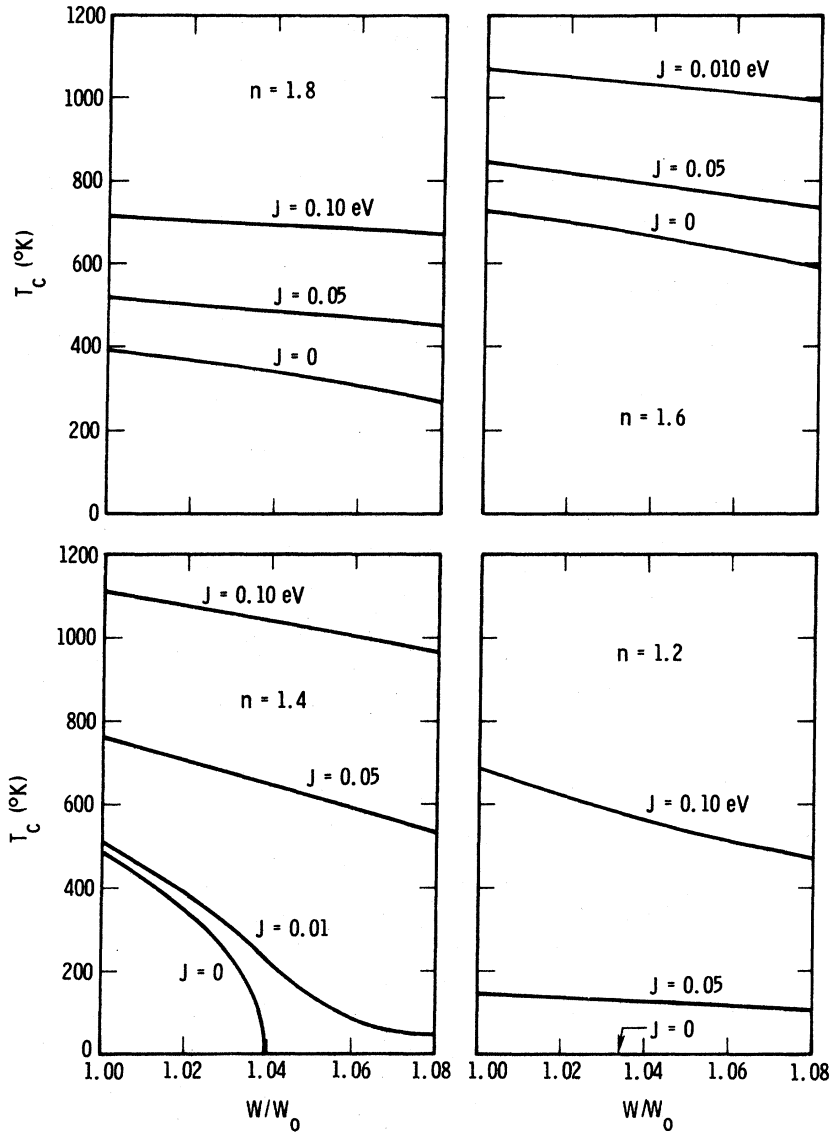

FIG. 7. Calculations of T_C as a function of W/W_0 for various J's and n's with $S=1$, $W_0=3.42$ eV, and $I=0.90$ eV. The concave upwards appearance of the $n=1.4$, $J=0.01$-eV curve is due to the T_C^{-1} term in I_{eff}.

of the T_C-vs-P data for MnSb is also consistent with the modified-Zener-model calculations with a small J.[10] The observed behavior of $\partial T_C/\partial P \sim -T_C^{-1}$ (for $P \to 0$) in Invar-type alloys[10,12,36] and transition-metal compounds[9,10] is consistent with the model calculations. In the weak-itinerant-electron theory for ferromagnetism,[7,9] $\partial T_C/\partial P = -\text{const}/T_C$; integrating this expression gives $T_C(P) = T_C(0)\,(1 - P/P_c)^{1/2}$, where $T_C(0)$ is T_C at $P = 0$ and P_c is the critical pressure (the FM state vanishes for $P > P_c$).[36,37] This expression for T_C agrees with the expression for T_C as a function of W used in the discussion of the Mn-substituted Invar alloys.[10] In the limit $P \to 0$, P_c can be determined from the initial slope, $P_c = -\frac{1}{2} T_C(0)/(\partial T_C/\partial P)$. For Invar P_c is predicted to be 76 kbar, and for $x = 0.09$, 0.16, and 0.19 in the Mn-substituted Invar alloys, P_c is predicted to be 44, 25, and 19 kbar, respectively.[10] These predictions are in sharp contrast to experimental results.[10] It is noteworthy that in $ZrZn_2$, a material which is thought to be the epitome of a weak-itinerant-electron ferromagnet, the P_c calculated from the initial values[37,38] of T_C and $\partial T_C/\partial P$ is approximately 6 kbar; whereas, experimentally it is observed that T_C decreases linearly with increasing P to 7.5 kbar and the FM state vanishes almost catastrophically between 7.5 and 8.5 kbar. (The curve that Smith *et al.*[37] used to fit their experimental data does not yield the observed initial slope.)

For the materials discussed above, with the possible exception of MnSb, the P dependence of T_C to high pressure cannot be described by the Stoner-Wohlfarth theory, at least in its elementary form.

However, the experimental data are consistent with the results of the model calculations shown in Figs. 5–7. It would appear that an appropriate model for ferromagnetism in the Invar-type alloys and possibly $ZrZn_2$ is a system of localized spins coupled via itinerant electrons such as in the Zener model. Although a detailed comparison of experiment and theory has not been made, it is clear the modified Zener model would be capable of explaining the pressure results. In order to test the applicability of the theory, further experimental work on the P dependence of T_C and a search for the optic branch of the spin-wave spectrum are needed.

In conclusion, the model calculations of T_C, based on the modified Zener model for ferromagnetism, are consistent with experimental observations in some transition metals, alloys, and compounds. To describe the FM behavior of an alloy system, e.g., the Fe-Ni alloy system, detailed calculations of the effective exchanges I and J and the effective number of itinerant d electrons per atom are needed. At low temperatures the mean-field value of I_{eff} diverges and the self-energy-type terms are important and should be included in the calculation of I_{eff}. The excitation spectrum (Fig. 1) has some interesting features and further experimental and theoretical work would be fruitful. To complete the picture of the modified Zener model for ferromagnetism, model calculations of the spin-wave behavior and the low-temperature behavior of the magnetization as a function of temperature and pressure are planned.

ACKNOWLEDGMENT

The author wishes to acknowledge Dr. H. S. Jarrett for stimulating discussions concerning itinerant-electron ferromagnetism and helpful comments on the manuscript.

*Work supported by the U. S. Atomic Energy Commission.

[1]C. Herring, in *Magnetism*, edited by G. T. Rado and H. Suhl (Academic, New York, 1966), Vol. IV, pp. 123–125 and 182–186.

[2]E. C. Stoner, Philos. Mag. **19**, 565 (1935).

[3]E. P. Wohlfarth, J. Appl. Phys. **39**, 1061 (1968).

[4]E. P. Wohlfarth, J. Phys. C **2**, 68 (1969).

[5]M. Shiga, Solid State Commun. **7**, 559 (1969).

[6]D. M. Edwards and E. P. Wohlfarth, Proc. R. Soc. A **303**, 127 (1968).

[7]J. Mathon and E. P. Wohlfarth, Phys. Status Solidi **30**, K131 (1968); E. P. Wohlfarth, Phys. Lett. A **28**, 569 (1969); Phys. Lett. A **31**, 525 (1970).

[8]E. P. Wohlfarth and L. C. Bartel, Phys. Lett. A **34**, 303 (1971).

[9]L. R. Edwards and L. C. Bartel, Phys. Rev. B **5**, 1064 (1972).

[10]L. C. Bartel, L. R. Edwards, and G. A. Samara, in *Proceedings of the Seventeenth International Conference on Magnetism and Magnetic Materials, No. 5*, edited by C. D. Graham, Jr. and J. J. Rhyne (AIP, New York, 1972), pp. 482-486.

[11]J. Kanamori, Prog. Theor. Phys. **30**, 275 (1963).

[12]R. C. Wayne and L. C. Bartel, Phys. Lett. A **28**, 196 (1968).

[13]J. Hubbard, Proc. R. Soc. A **276**, 238 (1963).

[14]E. Lieb and D. Mattis, Phys. Rev. **125**, 164 (1962).

[15]T. Arai and M. Parrinello, Phys. Rev. Lett. **27**, 1226 (1971).

[16]C. Zener, Phys. Rev. **82**, 403 (1951).

[17]T. Kasuya, Prog. Theor. Phys. **16**, 45 (1956).

[18]D. M. Edwards, Phys. Lett. A **33**, 183 (1970).

[19]P. W. Anderson and H. Hasegawa, Phys. Rev. **100**, 675 (1955).

[20]R. Harris and M. J. Zuckerman, Phys. Rev. B **5**, 101 (1972).

[21]H. Hasegawa and J. Kanamori, J. Phys. Soc. Jap. **31**, 382 (1971).

[22]D. N. Zubarev, Usp. Fiz. Nauk **71**, 71 (1960) [Sov. Phys.-Usp. **3**, 320 (1960)].

[23]S. Doniach and E. P. Wohlfarth, Proc. R. Soc. A **296**, 442 (1967).

[24]T. Izuyama, D. Kim, and R. Kubo, J. Phys. Soc. Jap. **18**, 1025 (1963).

[25]H. S. Bennet and P. C. Martin, Phys. Rev. 138, A608 (1965).

[26]H. Falk, Phys. Rev. **165**, 602 (1968).

[27]R. M. Wilcox, Phys. Rev. **174**, 624 (1968).

[28]P. A. Wolff, Phys. Rev. **120**, 814 (1960).

[29]For example, see M. Hatherly, K. Hirakawa, R. D. Lowde, J. F. Mallett, M. W. Stringfellow, and B. H. Torrie, Proc. Phys. Soc. Lond. **84**, 55 (1964); G. Shirane, V. J. Minkiewicz, and R. Nathans, J. Appl. Phys. **39**, 383 (1968); F. Menzinger, G. Caglioti, G. Shirane, R. Nathans, S. J. Pickart, and H. A. Alperin, J. Appl. Phys. **39**, 455 (1968); H. A. Mook, R. M. Nicklow, E. D. Thompson, and M. K. Wilkinson, J. Appl. Phys. **40**, 1450 (1969). In this last reference, the spin-wave spectrum for Ni was measured to 0.12 eV, and the "entering" of the spin waves into the Stoner continuum was observed. Since the modified Zener model may not apply to Ni metal, see Refs. 1 and 15, there may not be an optic branch; none was observed.

[30]A Sommerfeld expansion of the type used in Refs. 3, 4, 6, 9, and 10 could be employed and the result would be a cubic equation for T_C. In this work Eq. (32) will be solved using a particular $N(\epsilon)$.

[31]M. E. Lines, Phys. Rev. 135, A1336 (1964).

[32]V. Heine, Phys. Rev. **153**, 673 (1967).

[33]This expression for $N(\epsilon)$ can be obtained from the single-particle GF, neglecting the exchange interactions, using Eqs. (11) and (12).

[34]P. W. Anderson, Phys. Rev. **124**, 41 (1961).

[35]D. R. Penn, Phys. Rev. **142**, 350 (1966).

[36]J. M. Leger and C. Susse-Loriers, Phys. Lett. A **37**, 145 (1971).

[37]T. F. Smith, J. A. Mydosh, and E. P. Wohlfarth, Phys. Rev. Lett. **27**, 1732 (1971).

[38]R. C. Wayne and L. R. Edwards, Phys. Rev. **188**, 1042 (1969).